Mega Reclamation Projects: Challenges and Lessons Learned in Soil Improvement Works and Acceptance Tests

K. Yee[1] and S. Varaksin[2]
[1]*Association of Geotechnical Societies in South East Asia (AGSSEA), Kuala Lumpur, Malaysia*
[2]*Apageo, Paris, France*
E-mail: kenny.yeeks@gmail.com[1] / s.varaksin@apageo.com[2]

ABSTRACT: Singapore is the world's second busiest port with an average of 60 vessels calling daily. As a testament to Singapore's commitment to maintain its position as a global maritime nation, the government is going full steam ahead with the multi-billion dollars mega-port terminal development at Tuas. The Tuas Terminal will be developed in four phases over 30 years. Phase 1 reclamation of 294 hectares began in 2016 while the works contract for Phase 2 reclamation of 387 hectares was recently awarded in February 2018. When this entire development is completed by 2040, it is expected to be the largest container terminal in the world. For the land-scarce small city-state, creating new land by reclaiming it from the sea has played an important role in the country's maritime industry. Its first reclamation project for terminal development was in 1967. This was followed by a string of reclamation projects including Tanjong Pagar Terminal (80 hectares), Keppel Terminal (105 hectares), Brani Terminal (84 hectares) and Pasir Panjang Terminal (456 hectares). While it continues to develop and expand its maritime industry, it faces serious challenges to land reclamation due to limited availability of sand, among others. As sand is not readily available in large quantity, it calls for innovative solutions to overcome material constraint. Prior to Tuas, in another mega terminal development which was completed in 2015, the use of alternative reclamation fill materials was initiated to replace sand. Dredged materials from deepening of basins and nearby fairway as well as excavated earth from land construction projects were reused as reclamation fill materials. The use of these alternative materials, which would otherwise be disposed of, managed to save 45% in sand volume and saved SGD470 million construction cost. Also, it reduced the need for disposal grounds for the dredged and excavated materials. Needless to say, the innovations first deployed in this development are now being implemented to a greater degree in the upcoming Tuas Terminal. The concept and application of the innovations used in this earlier terminal development are presented as a case study in this paper. This paper describes some of the soil improvement techniques and acceptance tests used and it highlights the challenges and lessons learned.

Keywords: Land reclamation, Vibro compaction, Dynamic compaction, Dynamic replacement, Pressuremeter test, Cone penetration test.

1. INTRODUCTION

When Singapore gained independence in 1965, it was a low-income country with limited natural resources that lacked basic infrastructure. A few decades later, the picture could not be more different. Today, the small city-state is the world's second busiest port after Shanghai. It is no surprise that Shanghai is the number 1 busiest port given that China has a massive population of 1.3 billion and it has the largest economy in the world – when measured in terms of gross domestic product (GDP) based on purchasing-power-parity (PPP). According to IMF's World Economic Outlook, April 2017, China's GDP of US$23.19 trillion exceeds the U.S. GDP of US$19.42 trillion. The economic strength of China is supported by the fact that seven of the world's top ten busiest ports are in China.

Maritime is steeped in the lifeblood of Singapore, with its illustrious relationship tracing back to its humble beginning as a fabled and historic port-of-call and entrepôt. After playing a critical role in the country's development from a third world to a first world nation within one generation, the maritime sector continues to be a significant engine of growth for the country's economy, making up 7% of the country's GDP and employing more than 170,000 people. Singapore accounts for one-seventh of the world's container shipments and it is one of the world's largest refrigerated container ports with connections to 600 ports in over 120 countries. It trans-ships a fifth of the world's shipping containers. In 2017, the port handled over 33.67 million TEUs (Twenty-foot Equivalent Units) only losing to Shanghai's 40.23 million TEUs but exceeds Shenzhen, China (25.21 million TEUs); Ningbo-Zhoushan, China (24.61 million TEUs); Busan, South Korea (21.40 million TEUs); Hong Kong (20.76 million TEUs); Guangzhou, China (20.37 million TEUs); Qingdao, China (18.26 million TEUs); Dubai, UAE (15.44 million TEUs); and Tianjin, China (15.21 million TEUs) – thus, making up the world's top ten busiest ports in 2017.

Singapore's achievements did not happen by chance but based on forward-looking policy. To maintain its position and to stay ahead of the competition, the government has carried out a series of bold moves by building ahead of demand. Starting with the opening of the Tanjong Pagar Terminal in 1972, it made waves not just as the country's first container terminal, but also as the first in Southeast Asia. By 1982, it achieved 1 million TEUs in a year for the first time, and Singapore became the world's busiest port by shipping tonnage. In 1990, it crossed the 5 million TEUs mark and became the world's largest container port for the first time. Further expansion led to the opening of Keppel Terminal in 1991 and Brani Terminal in 1992. By 1994, Singapore achieved 10 million TEUs.

With the container handling volume growing exponentially worldwide, shipping lines have been increasing the size of their ships, doubling in size every eight years over the last two and a half decades. Recognising the need to ramp up capacity through larger cranes, deeper berths and longer quay lengths to serve mega ships that stretch over 400m in length and hold 18,000 standard-sized containers or more, the Pasir Panjang Terminal was opened in 2000. In 2005, Singapore surpassed 20 million TEUs in a year. Soon after, the government announced further expansion of Pasir Panjang Terminal. The Pasir Panjang Terminal Phases 3 and 4 were opened in 2015. In 2017, Singapore has handled over 33 million TEUs.

Today, Singapore has once again betting big on future trends that make or break economies – to develop a mega-size technologically advanced container terminal. It is one of the country's most ambitious projects yet, aimed at almost doubling the 33 million TEUs in 2017. The multi-billion dollars Tuas Terminal is a major milestone in Singapore's next generation container terminal development. It is set to be a showcase for the latest port technology and systems. This development will be carried out in four phases over 30 years. Works for Phase 1 reclamation of 294 hectares started in 2016. The works contract for Phase 2 reclamation of 387 hectares was recently awarded in early 2018. When the entire development is completed by 2040, it is expected to be the largest container terminal in the world with a total handling capacity of up to 65 million TEUs annually – more than the combined 50 million TEUs capacity of the current terminals at Tanjong Pagar, Keppel, Brani and Pasir Panjang. When Tuas Terminal is completed, all the current terminals will relocate and merge at Tuas. This consolidation of container port activities will not only result in increased efficiency in port operations due to the elimination of inter-terminal haulage but also free up 925 hectares of waterfront land for development. Figure 1 shows an artist's impression of the Tuas Terminal.

Figure 1 Artist's impression of the Tuas Terminal

Yet challenges loom: While Singapore continues to develop and expand its maritime industry, the small city-state faces yet another challenge – finding land for developments. Land is Singapore's most cherished resource and its dearest ambition. Past terminal developments were all built on reclaimed land; including Tanjung Pagar Terminal on 80 hectares of reclaimed land, Keppel Terminal on 105 hectares of reclaimed land, Brani Terminal on 84 hectares of reclaimed land and Pasir Panjang Terminal on 456 hectares of reclaimed land (Figure 2). The upcoming Tuas Terminal Phases 1 and 2 also involve the reclamation of 294 and 387 hectares of land respectively. Since the first reclamation works began in 1822, Singapore's land area has expanded by a whopping 25% from 58,150 to 71,910 hectares in 2017. In its 2013 Land Use Plan, the government has set a goal to reach a total land size of 76,600 hectares by 2030 for its planned developments – meaning Singapore still has some growing to do.

Figure 2 Reclaimed land for terminal developments

But there are serious challenges to land reclamation for the small city-state – the availability of sand for reclamation. The problem is Singapore has used so much sand that it has run out of its own, and need to import sand from elsewhere to meet its massive land reclamation needs. Skyrocketing price of imported sand just added fuel to the fire. The situation got worst when Malaysia banned the export of sand to Singapore in 1997; followed by Indonesia in 2007 and Vietnam in 2009. In 2016, Cambodia enacted a ban against exporting sand to Singapore. Hence, aggressive land reclamation programme using sand is no longer tenable. It calls for innovative solutions to overcome material constraint.

In 2015, a mega terminal development was completed using several innovative engineering solutions including the use of alternative reclamation fill materials to replace sand. Dredged materials such as marine clay from deepening of basins and nearby fairway as well as excavated earth from land construction projects (e.g. roads, MRT, etc.) were reused as reclamation fill materials (Figure 3). The use of these alternative materials, which would otherwise be disposed of, managed to save 45% in sand volume and saved SGD470 million construction cost. Also, it reduced the need for disposal grounds for the dredged and excavated materials

Drawing upon the lessons and experiences gained from this development, reusing alternative materials is expected to reduce the quantity of sand required by up to 60% and will result in a potential cost savings of some SGD1 billion in the upcoming Tuas Terminal. Needless to say, the innovations first deployed in this development are now being implemented to a greater degree in Tuas.

The concept and application of the innovative solutions used in this mega terminal development are presented as a case study in this paper. This paper describes the reclamation activities and some of the soil improvement techniques and associated acceptance tests used. It highlights the challenges and lessons learned.

Figure 3 Transportation of dredged materials by barges (top) and dredged clay lumps (bottom)

2. CASE STUDY: PROJECT DESCRIPTION

Singapore's Prime Minister Lee Hsien Loong opened this SGD3.5 billion mega terminal development in June 2015. Figure 4 shows the aerial photograph of the new terminal built on 198 hectares of reclaimed land. It consists of 15 deepwater container berths on 6,000m of quay length and up to 18m draft, designed to serve mega container ships with capacities larger than 10,000 TEU. It has container yard equipped with intelligent planning and operation systems, as well as unmanned rail-mounted gantry cranes. With the full operation of this terminal, it boosts Singapore's annual handling capacity by 40% to 50 million TEUs.

Figure 4 Aerial view of the new terminal development

Construction works began in 2007. It showcased several innovative engineering feats that were recognised for engineering achievements thought to have the greatest economic, infrastructural and societal impact. In 2016, it was voted by the public as being one of Singapore's Top 50 Engineering Achievements – making it a construction model for the upcoming Tuas Terminal.

Some of the innovative engineering solutions used during reclamation works include the use of large concrete blocks (caissons) to build the seawall and wharf structure instead of traditional piling methods and the use of alternative reclamation fill materials instead of sand. The construction works was completed in 2015 and the terminals are in full operation since 2017. Figure 5 shows the key reclamation activities that happened simultaneously and they are:

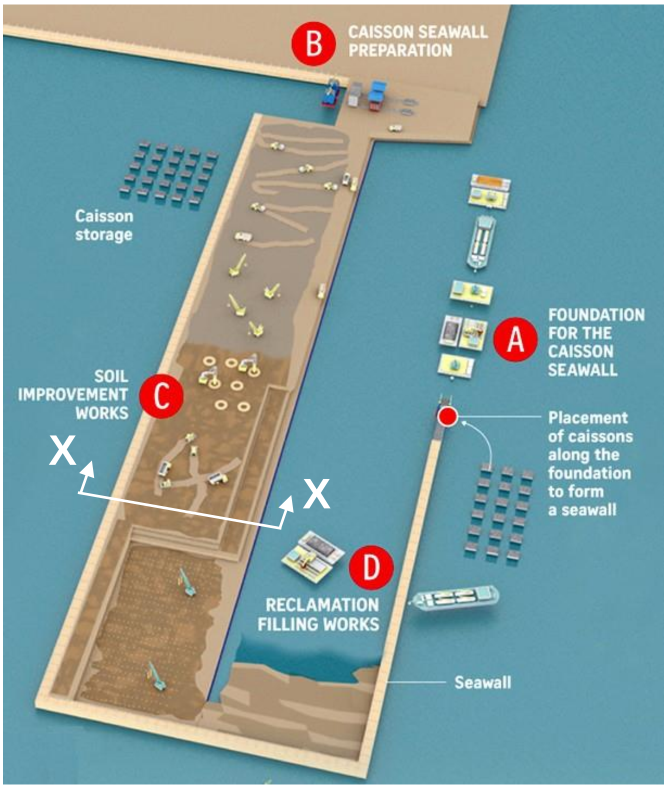

Figure 5 Reclamation activities (source: The Straits Times on 28-10-2016)

a) Activity A: Laying foundation for the caisson seawall.
   Soft clay was dredged from the seabed until the hard strata to form sandkey trench. Sand was filled into the trench and compacted. After sand compaction, rocks were laid and subsequently compacted to form rock mound.
b) Activity B: Caisson seawall preparation and placement.
   The construction of caisson units consisted of (i) casting of base slab; (ii) casting of caisson wall; (iii) curing of completed caisson unit; and (iv) towing of caisson unit out to sea and ready for installation.
c) Activity C: Soil improvement works.
   Vertical drains were used for the improvement of dredged materials and excavated earth. They were installed to depths up to 55m. Some 24 million meters of vertical drains were installed. After installation of vertical drains, sand surcharging was carried out to a fill height of 18m. After removal of surcharge fill, deep compaction was carried out to compact the sand fill using vibro compaction and dynamic compaction. Thereafter, surface roller compaction was carried out on the good earth layer.
d) Activity D: Reclamation filling works.
   Alternative fill materials (i.e. dredged materials from sandkey trenches, deepening of fairways and basins; and excavated earth materials from land-based construction projects such as roads, MRT, etc.) were used as reclamation fill materials in addition to sand. Cemented-mixed soil was also used for the construction of the "geo-bund" temporary edge structure. The "geo-bund" provided the necessary safety benefits for the adjacent dredging work and construction of caisson seawall.

Taking a cross-section X-X from Figure 5, Figures 6 and 7 show the extent of the soil improvement works and the different reclamation fill materials used respectively. Using these alternative fill materials reduced the quantity of sand required by 45% and resulted in cost savings of SGD470 million.

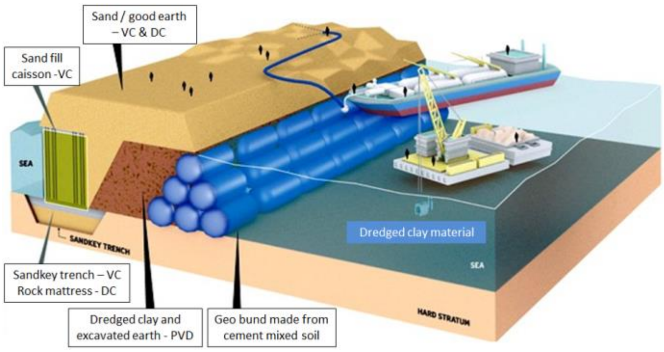

Figure 6 Extent of soil improvement works (PVD – vertical drains; VC – vibro compaction; and DC – dynamic compaction) (adapted from The Straits Times on 28-10-2016)

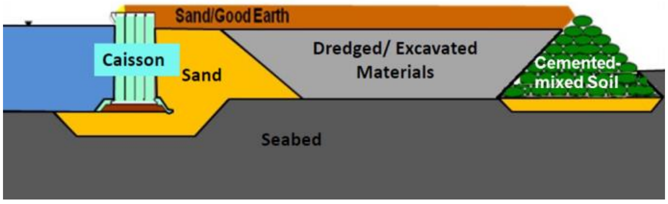

Figure 7 Usage of different reclamation fill materials

3. OFFSHORE SOIL IMPROVEMENT BELOW WATER

3.1 Caisson Seawalls

The reclamation works was designed based on the use of large reinforced concrete caissons to form seawalls. The caisson seawalls serve to retain the reclamation fill materials forming the land and to function as the quay for the container vessels when the berths are put into operation. The construction involved precasting the caissons using specialised machine and transporting the completed caissons into docking position using a floating dock. As the caissons were of standard sizes, an on-site fabrication yard was set up to allow round-the-clock concreting work. Under a factory-like environment, the productivity and works quality of the caissons were increased. One hundred and fifty caissons were constructed; each measuring 21 to 32m in height and weighs between 8,800 tonnes to 12,000 tonnes. These caissons were among the largest in the world. Figure 8 shows some of the completed caissons at the fabrication yard.

Figure 8 Completed caissons at the fabrication yard

3.2 Caisson Seawall Foundation: Construction, Design and Performance Requirements

The caisson seawalls were installed on rock (rubble) mound founded on sandkey trench (Figure 9). The foundation works consisted of (i) dredging of sandkey trench to reach very stiff strata; (ii) filling sandkey trench with sand followed by deep compaction; (iii) carrying out hydrographic survey after sand trimming and levelling; and (iv) placing rocks to form rock mound followed by compaction.

After completion of the foundation works, acceptance tests were carried out. Upon achieving the acceptance criteria, the caissons were installed, backfilled with sand and compacted.

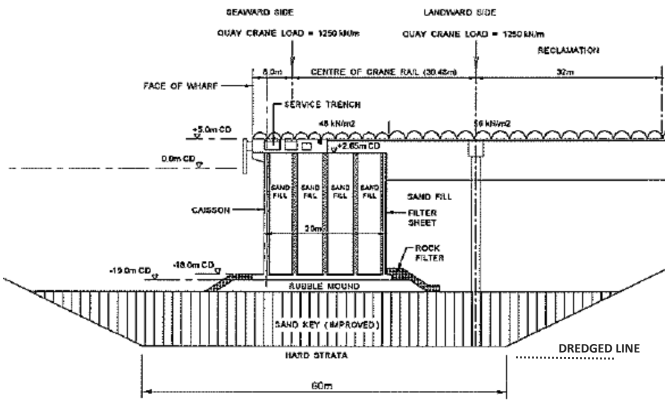

Figure 9 Cross-section of caisson on sandkey trench

The performance requirement for the foundation of the caisson seawalls was a residual settlement after construction not exceeding 40mm. To achieve this requirement, the construction of the sandkey trench called for complete removal of the underlying soft to firm clay until very stiff clay strata (undrained shear strength (c_u) of not less than 250 kN/m^2) and total replacement with clean sand. The sand fill with fine content (soil particles finer than 75μm) less than 10% was then compacted to achieve a relative density of minimum 70%. The design requirement was an internal angle of friction (ϕ) greater than 35^o and the acceptance criteria based on cone penetration tests (CPT) were cone resistance (q_c) of 8 MPa at the surface (i.e. top finished level of sandkey trench) increasing to 22 MPa at depth greater than 20m.

Deep vibro compaction was carried out to compact the sand fill. Vibroflots with maximum centrifugal force of 35.4 tons and amplitude of 26mm at the tip were used. The compaction was carried out with a 3m overburden sand fill placed above the top finished level of the sandkey trench. The compaction spacing was 3.5m triangular grid with compaction duration of 40 seconds at every 0.5m vertical lift increments.

After completion of vibro compaction and sand trimming, rocks of maximum 300mm size were placed to form mound ranging from 1 to 4m thick. The rock pieces were compacted to achieve design requirement of an internal angle of friction (ϕ) greater than 45^o.

3.3 Unexpected Soil Softening

Prior to the removal of the overburden sand fill after vibro compaction and before placing of the rock mound, CPT tests were carried out as routine acceptance tests. On a particular area at water depth of about 30m, non-compliance results (i.e. measured cone resistances lower than acceptance values) were recorded. Figure 10 shows a set of non-compliance CPT results after compaction.

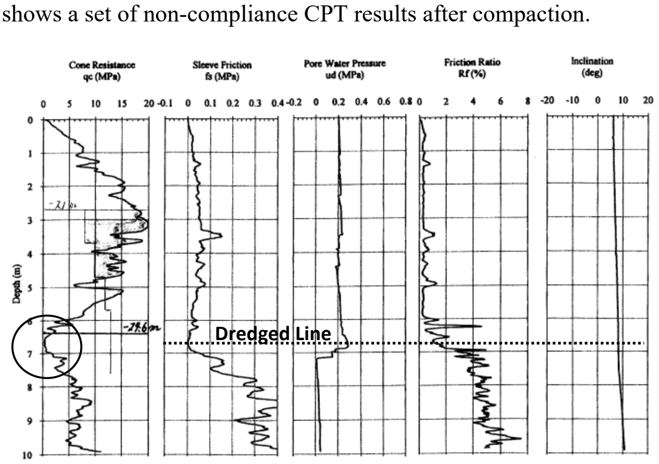

Figure 10 CPT results after vibro compaction of sandkey

The results revealed a layer of "softened" sensitive soil of about 1.5m thick at the base of sandkey trench and dredged seabed. To supplement the CPT tests, pressuremeter (PMT) tests were carried out on jack-up pontoon at 15 different locations. The tests were carried out in the sand fill and clay layer down to 33m or more below water. A summary of the PMT results is shown in Table 1.

The E_P/P_L ratios of the disturbed materials (i.e. disturbed sand / softened clay) were generally less than 7 indicating an altered or disturbed state while the undisturbed stiff clay shows a ratio greater than 16 indicating an over-consolidated state (D.60.AN, 1975).

Table 2 shows the estimated strength values – internal friction angle (ϕ) and undrained shear strength (c_u) of the materials based on PMT results of Table 1. The internal angle of friction (ϕ) of 30^o to 32^o for disturbed sand was less than the design requirement of 35^o while undrained shear strength (c_u) of 50 to 80 kN/m^2 for softened clay was also less than the design requirement of 250 kN/m^2. Only the undisturbed stiff clay layer registered undrained shear strength (c_u) greater than the design requirement. These values of ϕ and c_u were estimated from the equations below (Amar *et al*, 1991):

$$c_u = \frac{P_L *}{5.5} \qquad (1)$$

$$P_L^* = 2.5 * 2^{\left(\frac{\varphi^o - 24^o}{4}\right)} \qquad (2)$$

where P_L* is the net limit pressure (in bars) which is equal to the difference between the measured limit pressure (P_L) and the horizontal pressure at rest.

Table 1 Results of PMT tests after vibro compaction of sandkey

Material	E_P (MPa)	E_Y (MPa)	P_L (MPa)	E_P/P_L
Disturbed sand	2.6 – 3.3	7.8 – 9.9	0.70 – 0.72	3.8 – 4.4
Softened clay	0.7 – 1.2	1.4 – 2.4	0.49 – 0.51	1.5 – 2.3
Undisturbed stiff clay	36 – 39	36 – 39	2.05 – 2.26	17 – 18

Table 2 Estimated ϕ and c_u after vibro compaction of sandkey

Material	E_P/P_L	ϕ (^{o})	c_u (kN/m^2)
Disturbed sand	3.8 – 4.4	30 – 32	
Softened clay	1.5 – 2.3		50 – 80
Undisturbed stiff clay	17 – 18		> 250

Note: E_P is the pressuremeter modulus; E_Y is the stiffness modulus; P_L is the limit pressure; ϕ is the internal angle of friction and c_u is the undrained shear strength.

3.4 Remedial Solution

From the CPT results, the total thickness of disturbed sand and softened clay layer ranged from 80 – 150cm. Based on the measured "c-ϕ" values, a re-analysis was carried out for caisson seawall settlement and stability. Figure 11 (left) shows the original design assumptions (design requirements) compared to the measured field values in Figure 11 (center). To meet the performance requirement, it was necessary to reinstate ("improve") the measured field strength values back to the original design assumptions or equivalent. Figure 11 (right) shows the "target" revised design requirements.

A remedial solution consisted of a rock mat over reinforcing rock columns was adopted. Rock columns were introduced to improve the composite strength properties (c-ϕ) of the softened clay while the compacted rock mat was introduced to increase the internal angle of friction (ϕ) of the disturbed sand. It also served as a load distribution layer to the reinforcing columns below. Dynamic replacement was carried out to install the rock columns and dynamic compaction was carried out to compact the rock mat.

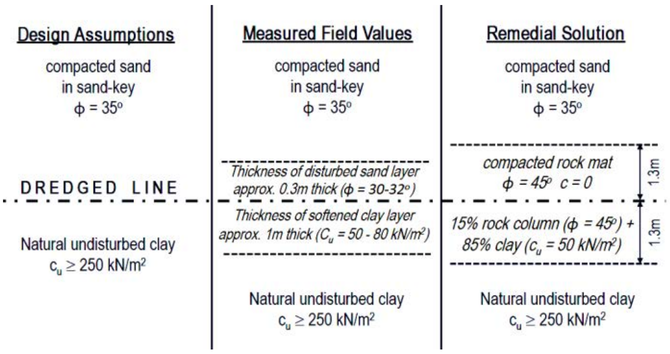

Figure 11 Comparison of design, average field and target values

3.5 Principle of Dynamic Compaction / Dynamic Replacement

Dynamic compaction is a soil improvement technique used for in-situ densification (compaction) of granular soil (e.g. sand) by heavy impacts. It is done systematically in a pre-determined grid pattern. It consists of delivering high energy impacts at the ground surface by repeatedly dropping 10 to 40-ton steel pounder from heights of 10 to 40m using a crane (Figure 12). Deep craters up to 2m are formed as a result of the impacts. In loose sand, the heave around the craters is generally small. The craters are filled with sand after each phase.

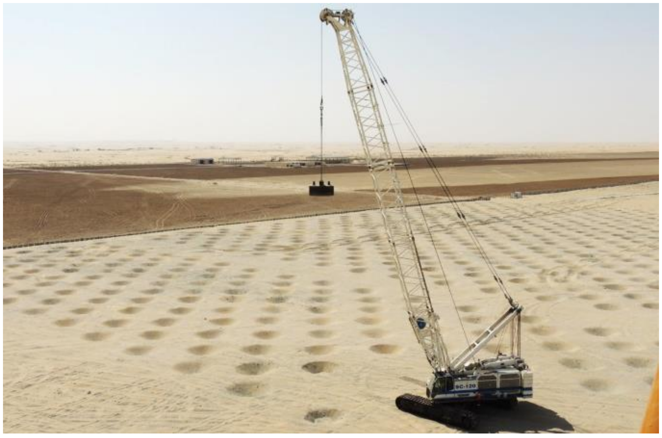
Figure 12 Dynamic compaction rig and impact craters

The spacing between compaction points depends on the required depth of compaction, grain size distribution, permeability and location of the ground water table. The initial spacing of the compaction points roughly corresponds to the compaction depth. It is necessary to use highest compaction energy, with the heaviest pounder falling from maximum drop height for the early phases of compaction in order to extend the compaction effect as deep as possible. The compaction energy and the spacing of compaction can then be reduced for subsequent phases thereby allowing adequate compaction to be carried out at shallower depths (Figure 13).

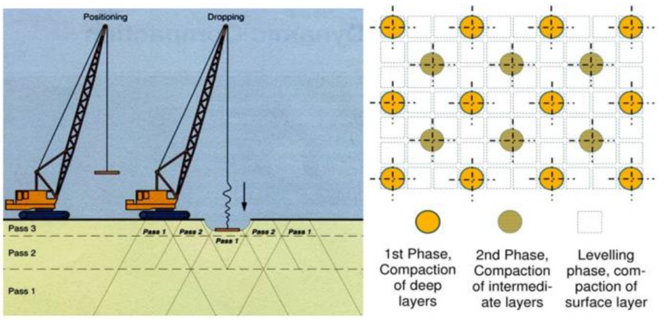

Figure 13 Different phases of dynamic compaction

Empirical formulae for the estimation of depth of improvement (D) and the degree of improvement relative to the depth (F_Z) are given below (Varaksin and Racinais, 2009):

$$D = n.\sqrt{W.H} \tag{3}$$

$$F_z = \frac{F_2 - F_1}{D^2}\left(Z - Z_o\right)^2 + F_1 \tag{4}$$

where D = depth of improvement / compaction (m)
W = weight of pounder (ton)
H = drop height (m)
n = constant (depending on soil type, degree of saturation)
F_Z = improvement ratio at elevation z
F_1 = maximum improvement ratio at surface
F_2 = improvement ratio at depth of compaction
Z = elevation (m)
Z_o = natural (original) ground level (m)

The compaction is generally the highest below the pounder. Maximum increase in density is at about one third of the depth of compaction from the surface. An increase of the penetration resistance of 300 to 400% can be expected in clean sand and gravel.

Dynamic replacement provides an alternative to dynamic compaction when the saturated soil cannot be compacted due to low permeability or excessive fine contents – generally greater than 10 – 15%. Dynamic replacement is an extension of dynamic compaction, using similar plant and equipment (Figure 14). However, unlike dynamic compaction which is a soil densification technique for granular soil, dynamic replacement is a soil reinforcement technique used mainly for cohesive soil (e.g. clay). Stiffer materials with higher shear modulus are introduced into the soil mass as reinforcing columns. The improvement of the cohesive soil mass is derived from the structural aspect of the stiffer reinforcing columns via a composite soil-column mass, interacting through friction and adhesion. It increases the bearing capacity, reduces settlement and improves stability. Backfilling materials for the columns can be any free-draining, hard, durable, inert materials such as sand, stones or even rock pieces (up to 300mm size). The volume of columns usually represents about 15 – 25% of soil mass volume.

Dynamic replacement process starts out by producing a pilot crater ("print") with light pounding. The crater is then backfilled with suitable materials that will lock together under subsequent heavy pounding (Figure 14). This pounding process is repeated with increasing compaction energy until a noticeable decrease in crater formation occurs. Since the column material is more permeable, pore water pressure from the underlying and adjacent less permeable cohesive soil will dissipate quickly. Hence, the columns being load bearing columns (reinforcement) also serve as large vertical drains.

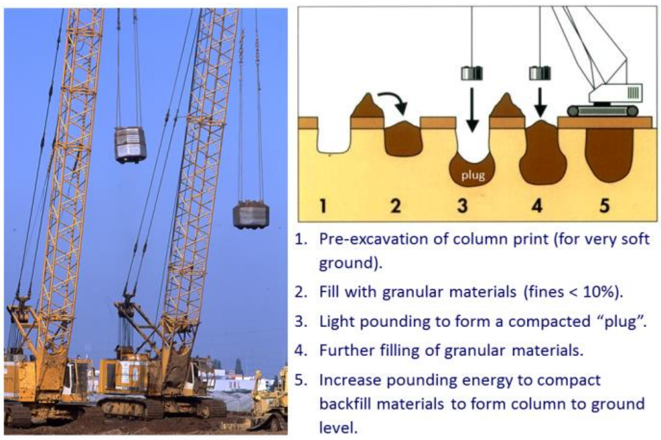

Figure 14 Dynamic replacement rig and works procedure

Column diameter up to 2.5 to 3m is common for dynamic replacement. The surface area of these columns is approximately 5 to 7 m² with design bearing capacity up to 100 tons per column in soft to medium stiff clay. Spacing of columns varies from 4.5 to 7m.

While dynamic compaction (DC) and dynamic replacement (DR) technique share similar plant and equipment, there are distinctive differences in their applications and works procedure:

a) DC creates a homogeneous soil compaction mass effect while DR is a composite soil-column reinforcement effect (Figure 15);
b) DC uses the same soil material for compaction while DR uses imported material "stiffer than the soil mass" for the columns;
c) DC starts with maximum compaction energy to reach design compaction depth and finished with reduced energy in the final ironing phase while DR starts with low compaction energy to form the column "plug" and finished with increased energy to compact the whole column material.
d) DC uses compaction pounder with larger surface area to avoid "punching" into the soil while DR uses a punching pounder with smaller surface area for more penetration effect (Figure 16).

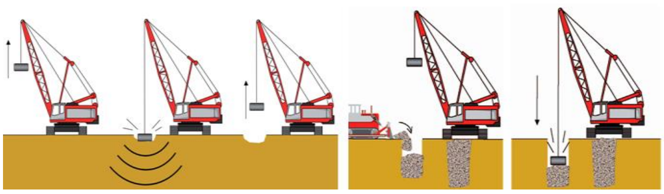

Figure 15 Mass compaction of dynamic compaction (left) and composite soil-column effect of dynamic replacement (right)

Figure 16 Punching DR pounder (left) and flat DC compaction pounder (right)

3.6 Offshore Dynamic Compaction / Replacement Works

To improve the disturbed soil layers, a working platform of 1.8m thick rock blanket was placed at the dredged line after removal of sand in the sandkey trench. For ease of compaction below water, granite rock pieces with 30% grading size between 150 to 200mm and 70% grading size between 200 to 300mm well-graded were used. Dynamic replacement (DR) process was first carried out on top of the rock blanket to form rock columns 1.3m into the softened clay layer. The rock columns were designed as 2m diameter columns installed at a square grid of 4.5m corresponding to an area replacement ratio of 15.5%. The compaction inside the rock columns was carried out to achieve an internal angle of friction (ϕ) of 45°. After completion of the DR process, the remaining rock blanket was compacted by dynamic compaction (DC) process to form the 1.3m thick compacted rock mat with an internal angle of friction (ϕ) of 45°. Both DC and DR works were carried out about 30m below water. Figure 11 (right) shows the mechanical properties to be achieved with this remedial solution. These targeted values were used to re-analyse the caisson seawall settlement and stability.

3.7 Field Calibrations

Prior to actual production works, several field calibrations (also known as field trials) were carried out to calibrate the field operation parameters with the "target" revised design requirements. Field performances were verified by field measurements of rock volume used; surface elevations before and after DC/DR compaction; and pressuremeter tests (PMT) before and after DC/DR compaction. Cone penetration test (CPT) was not carried out due to the presence of compacted rock and its grading sizes.

Since dynamic compaction and dynamic replacement were carried out below water, the conventional "solid" pounders shown in Figure 16 were not suitable due to water buoyancy. A special offshore pounder was designed and built for this purpose following a hydrodynamic impact study (Figure 17). The study was carried out to determine the impact speed below water; water resistance and inertia; impact stress and durability of the pounder while providing sufficient "punching" energy to create the rock columns and "compaction" energy to compact the rock mat.

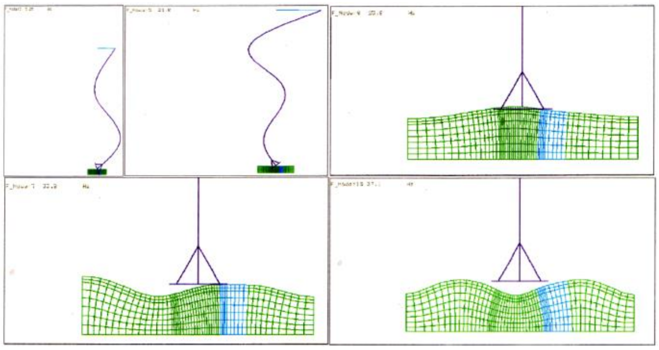

Figure 17 Hydrodynamic impact analysis of the offshore pounder

Based on the terminal velocity of 7 to 8 m/s obtained from the hydrodynamic impact study, the optimized configuration and shape of the offshore pounder is shown in Figure 18. It was a combined design of a "DC-and-DR" pounder in a single unit with two compaction "surfaces" – larger one for DC and smaller one for DR.

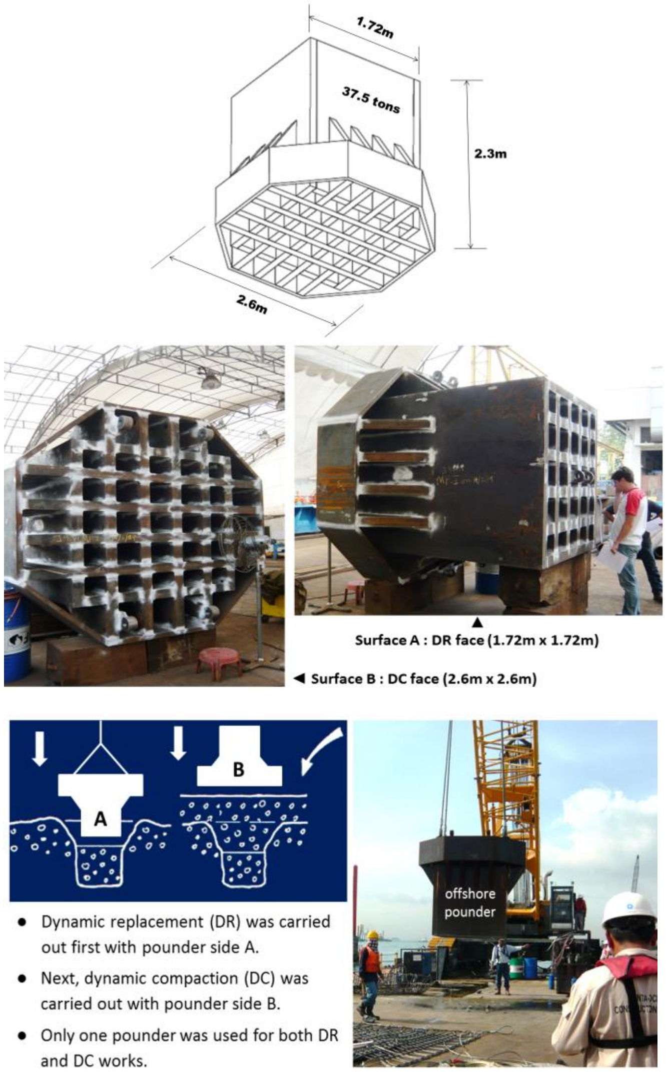

Figure 18 Offshore DC-DR pounder

The weight of the offshore pounder was 37.5 tons with its smaller "punching" surface area of 1.72m x 1.72m (approximately 3 m^2) for dynamic replacement process and a larger "compaction" surface area of 2.6m by 2.6m (approximately 6.8 m^2) for dynamic compaction process. The height of the pounder was fixed at 2.3m determined from the required DR columns penetration. The ratio of solid surface area over open surface area was determined based on minimum water resistance against net pounder weight. The pounder was made of special manganese steel plates to withstand the abrasion caused by the heavy impacts on the granite rocks.

Using this offshore pounder, field calibration tests were carried out on an area of 22.5m by 22.5m (506 m^2). Twenty-five test columns were installed at 4.5m square grid with 30 blows per column. The drop height was 5m in water. Drop height greater than 5m was shown not to improve significantly the compaction as terminal velocity of 7 – 8 m/s was reached. This was consistent with the results obtained from the hydrodynamic impact analysis. After the completion of the columns, the rock mat was compacted with 3 to 6 blows at an overlapping grid pattern as the final ironing phase.

Based on field measurements, the number of blows was plotted against column penetration as shown in Figure 19. During "column penetration" phase, the first 15 blows produced significant column penetration with an average of 1.3m. After the 15 blows, additional blows produced marginal penetration (< 10 cm). However, more blows were needed to increase the density (compactness) of the columns. During this "column compaction" phase, additional 13 to 15 blows were given until surface heaving around the columns was recorded.

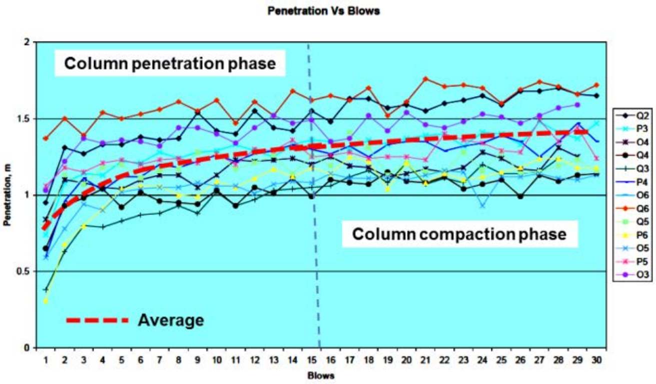

Figure 19 Column penetrations vs. number of blows

Pressuremeter tests (PMT) were carried out before DC/DR compaction works (pre-DC/DR tests). After compaction works, post-DC/DR PMT tests were carried out inside the DR columns and in-between the DR columns. During the tests, visual observation on the return of drilling fluid was recorded. When there was no return of drilling fluid, it confirmed that the PMT test was carried out within the confinement of the free-draining rocks (i.e. inside the DR columns). Otherwise, the PMT test was conducted in the impervious clay layer (i.e. in-between the DR columns) as indicated by the presence of returning drilling fluid due to undrained condition.

The average pre-DC/DR pressuremeter modulus (E_P) and limit pressure (P_L) for the uncompacted rock obtained from 9 different test locations were 2.4 MPa and 0.55 MPa respectively. The ratio of E_P/P_L was 4.4 (i.e. < 6 suggesting a loose state) (D.60.AN, 1975). The average post-DC/DR E_P and P_L values for the compacted rock obtained from 14 different test locations were 9.7 MPa and 1.2 MPa respectively. The ratio of E_P/P_L was 8.1 (i.e. > 6 suggesting a compacted self-bearing condition) (D.60.AN, 1975). The average estimated pre-DC/DR internal angle of friction of the uncompacted rock fill was about 42^o while the average post-DC/DR internal angle of friction of the compacted rock fill was about 48^o which exceeded the target value of 45^o.

The other physical measurements taken include:

- Total volume of loose rock pieces placed over the field calibration area of 506 m^2 was about 900 m^3. This is equivalent to 1.78 m^3 per m^2.
- Based on echo sounding survey before and after DC/DR works, the difference in measured surface elevations was about 38cm. Considering 1m^3 loose rock volume equivalents to 0.87m^3 compacted volume, the net enforced settlement was about 33cm. Hence, the calculated volume of a DR column was 6.7m^3 and the diameter of DR column was 2.5m.
- Based on sea-divers' "direct" field measurements, the diameter of the DR columns varied between 2.4 and 2.6m. These values are in agreement with the diagonal length (= 2.43m) of a 1.72m x 1.72m pounder – dimensions of the punching surface. Surface upheave of 10 – 20cm between the columns was recorded. The columns penetrated about 1.3m into the softened clay layer.

From these observations, the calculated and measured diameters of DR columns exceeded the target value of 2m. Hence, the field operation parameters were satisfactory for full production works. Figure 20 shows the probable soil profile before and after DC/DR works but before surface levelling. Due to larger columns, the area replacement ratio (ARR) had increased to 22% instead of 15.5%.

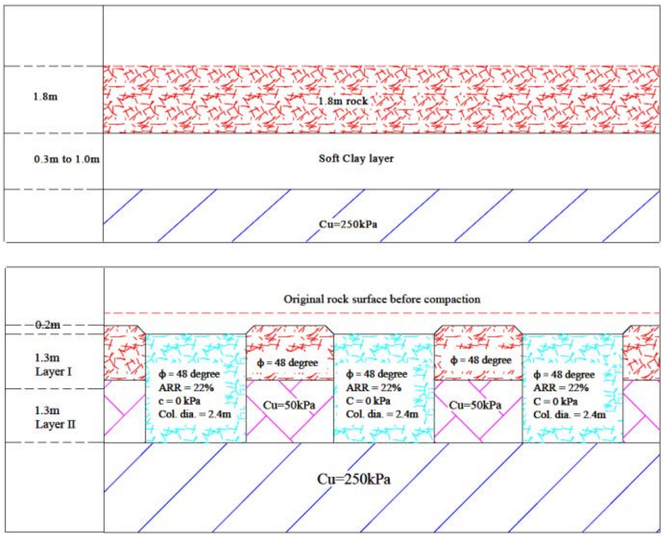

Figure 20 Probable profile before (top) and after DC/DR (bottom)

3.8 Execution of Full Production Works

With the completion of the field calibration tests, full production works was launched following the sequence below:

- Removal of sand from the sandkey trench.
  - Production rate for removing and dumping of sand was about 4,000 m^3 per day.
- Placement of 1.8m thick rock blanket as "working platform".
  - Well-graded granite rocks of 30% grading size between 150 to 200mm and 70% grading size between 200 to 300mm delivered by flat-top barges with tugboats equipped with excavators and shovels.
  - After completion of surface levelling and hydrographic survey, the rock pieces were placed using a tremie barge. The rock pieces were dropped down the tremie pipe and free-fall to the sea-bed. The depth of tremie pipe, tremie barge position and the quantity of placed rocks were monitored and controlled to achieve the intended coverage.
  - Soundings and interim hydrographic surveys were carried out regularly after rock placing.
  - Production rate for rock placing was about 3,000 m^3 per day.
- Installation of DR rock columns and compaction of rock mat.
  - The locations of DR columns were pre-determined and logged on to the GPS system located inside the DC/DR base crane cabin as part of the on-board computer system.
  - The DR columns were installed in two phases. The area coverage was divided into blocks and the installation of columns followed a zigzag line within each block.
  - The date, column position, initial and final rock elevations at each column locations were recorded by the on-board

computer system. Also, the operation parameters such as drop height, drop speed, impact velocity and number of drops at each column location; the total compaction time and the net "buoyancy" pounder weight were recorded.
  - Production rate was about 350 m^2 per day.
- Filling of sandkey trench with sand and subsequent compaction.
  - The sand filling proceeded immediately after compaction of the rock mat and acceptance tests.
  - The sand layer was compacted by vibro compaction.
  - Production rate was about 350 m^2 per day.
- Acceptance tests
  - Acceptance tests using PMT for compacted rock and CPT for compacted sand were carried out. PMT tests were carried out before and after DC/DR works. CPT tests were carried out after completion of vibro compaction works.
  - Visual inspections and field observations (including underwater inspections), surveys, samplings and testing were carried out at regular intervals.

The offshore DC/DR works was carried out using a 200-ton Liebherr LB895 hydraulic crane, fixed onto a crane barge measuring 25m by 50m with 4-point anchoring system. The DC/DR rig was equipped with GPS system and a quality control computer system for compaction. Figure 21 shows the plant and equipment used for the offshore DC/DR works. The works was completed in 2009.

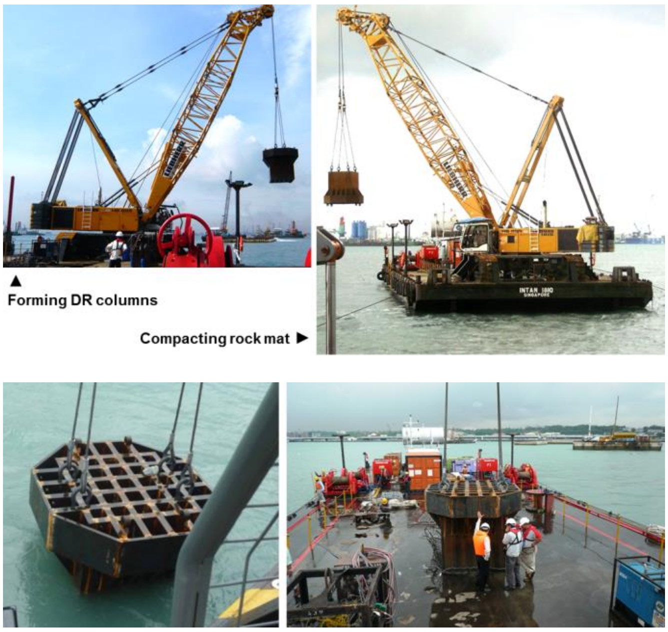

Figure 21 Offshore DC/DR rig on barge and offshore pounder

3.9 Post DC/DR Tests Results and Discussions

Settlement and stability for the caisson seawalls were re-analysed using the post-DC/DR strength parameters derived from PMT tests. PMT tests were carried out using the STAF system. STAF – self-bored tube system, is a slotted tube technique with inside disintegrating tool and mud circulation. This method emplaced the slotted casing tube while drilling to avoid borehole wall disturbance (Figure 22). This was deemed to bring improvement to the operation and the test results especially in non-homogeneous and over-consolidated soil. Figure 23 shows the PMT equipment deployed for the offshore testing works. PMT tests were carried out to depths of up to 33m below water on a jacked-up pontoon. After DC/DR works, PMT tests were carried out at 29 different locations which included both static and cyclic tests. A typical cyclic PMT test results is shown in Figure 24. A summary of the results is given in Table 3. Table 4 shows the ratio of the unload-reload pressuremeter modulus (E_{UR}) over the static pressuremeter modulus (E_P). The E_{UR}/E_P value ranged from 3.5 to 4.2 which agreed well with the suggested value of 3.5 – 4 for compacted rock and P_L greater than 0.8 – 1 MPa is adequate for self-bearing condition where settlement will not occur under its own weight (D.60.AN, 1975).

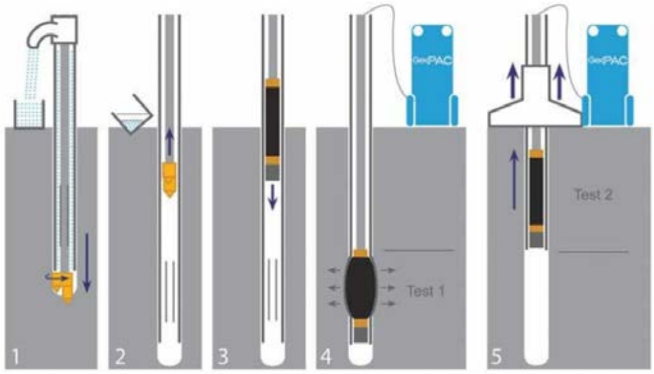

1. Self-boring with STAF bit – the eccentric tool bit drills at the bottom of the tube followed by the slotted tube to reduce wall disturbance. Drilling mud moves inside the tube and flows into a sediment tank for analysis.
2. Tool retrieval – the staf bit is pulled up inside the tube without any remolding of the borehole wall.
3. Probe positioning – the probe is located at the central of the steel strips forming the slotted tube.
4. Execution of the PMT tests
5. Extraction – test starts from the deepest level and moves up to the next testing level.

Figure 22 Operation of PMT test with STAF system

Figure 23 (a) PMT read-out unit; (b) PMT drilling rig; (c) jacked-up pontoon; and (d) STAF drill bit

Table 3 Results of PMT tests after DC/DR works

Material	E_P (MPa)	E_{UR} (MPa)	P_L (MPa)
Compacted rock	7.3 – 10.4	31 – 34	1.1 – 1.6

Table 4 Interpretation of PMT test results after DC/DR works

Material	E_P/P_L	E_{UR}/E_P	E_Y (Mpa)	ϕ (°)
Compacted rock	6.7 – 8.4	3.5 – 4.2	29 – 42	47 – 49

Note: E_P is the pressuremeter modulus; E_{UR} is the unload-reload pressuremeter modulus; E_Y is the stiffness modulus; P_L is the limit pressure and ϕ is the internal angle of friction.

The internal angle of friction ϕ (°) for the compacted rock was estimated based on the net limit pressure P_L* (bars) using the relationship below (Yee and Varaksin, 2012):

$$P_L^* = 4 * 2.5^{\left(\frac{\varphi - 40^o}{7}\right)} \tag{5}$$

Equation (5) is an extension of Menard (1970) equation for granular soil extending to $\phi > 40^o$; presumably the indicative lower bound value for the internal angle of friction (ϕ) for granite rock pieces of similar size which corresponds to measured P_L values of about 0.55 MPa (Varaksin, 2009).

The measured internal angle of friction (ϕ) of the rock after compaction was estimated to be between 47° and 49° with an average value of 48.5° based on an average P_L* of 1.2 MPa which satisfied the target requirement of 45°.

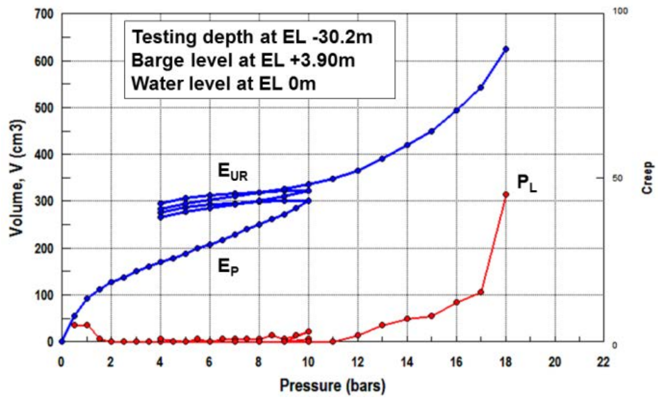

Figure 24 A typical cyclic PMT test results

3.10 Lessons Learned

Soil improvement on land above water is usually an easier task. When it is carried out at great depth below water, the task becomes more difficult. It requires more rigorous analyses and more elaborate construction procedure with specialized plant and equipment. The works procedure or methodology needs on-site adaptation to suit the prevailing conditions. Quality control becomes more critical as often, it is beyond our normal "visibility" range.

Some of the challenges and lessons learned in this offshore DC/DR works include:

- Adaptation of coarser and heavier backfill materials (i.e. rock instead of sand) for compaction under water due to water buoyancy and "turbulence" effect during impacts and the requirement to achieve a high internal angle of friction (ϕ);
- Adaptation of a "porous" and heavier DC/DR pounder for underwater compaction due to water buoyancy and terminal velocity of falling pounder and its limited drop height.
- Adaptation of appropriate quality assurance and quality control tests e.g. using PMT test for rock, cyclic and static PMT test to verify the compactness of rock pieces;
- Visual inspections and field observations above and below water (using sea divers) during works are necessary especially for offshore works to provide additional information to assess "what-is-going-on" below water.

4. ONSHORE SOIL IMPROVEMENT ABOVE WATER

4.1 Reclaimed Land behind Caisson Seawall

With the completion of the caisson seawall, sand was placed behind the seawall overlying the seabed. Further away from the seawall, dredged and excavated materials (alternative fill materials) were first placed on the seabed and followed by sand overlying it (Figure 7). The sand was obtained from marine borrow sources and transported to the reclamation site. The hydraulic placement of sand resulted in a loose state with CPT cone resistance (q_c) as low as 3 – 5 MPa. After sand filling, vertical drains were installed to accelerate the primary consolidation of the underlying cohesive materials followed by fill surcharge to reduce post construction settlement. Deep compaction was carried out after the removal of surcharge fill to densify the hydraulic sand fill to reduce creep and to mitigate vibration-induced settlement and liquefaction. Surface roller compaction was carried out for the upper layer of good earth.

4.2 Potential Problems of Loose Sand

D'Appolonia (1970) reported that loose sand is very unstable when subjected to even a modest shock and vibration. Such vibration could emanate from pile installation or from seismic effects. It is prone to liquefaction. For small strain of the order of 10^{-5} to 10^{-3} the minimum relative density to prevent liquefaction should be about 70% and that fine sand with a relative density less than 50% is subject to liquefaction during ground motions with acceleration in excess of 0.1g.

Hydraulic sand filling by pipeline method or rainbow method has large volume of water. The resulting fill structure is likely to be loose and it will remain loose because of the capillary retention of the sand which prevents the sand particles from rolling into a stable and denser configuration. Typical estimated relative density of sand fill above water level is 50% to 70% and below water level, it can be as low as 30% to 50%.

While loose sand is not as compressible as soft clay, it continues to settle under its own self-weight for many years after their initial deposition. Creep is often estimated as 1% of the thickness of loose sand fill per log cycle of time which is sufficiently large that it cannot be ignored in the design of foundations especially for thick fill as in this case study. Another inherent problem of loose sand is sudden instability. Although it may be metastable and change state readily, its very instability nature makes it possible to alter its loose structure effectively. Shearing of the sand particles by vibration or impact to form a denser and stable structure has been the most effective means for densifying loose sand.

Dynamic compaction and vibro compaction have found wide acceptance, and numerous case histories have illustrated their practical applications for densification of loose sand for higher bearing capacity and lower compression. Dynamic compaction has been described above. Vibro compaction is briefly described below.

4.3 Principle of Vibro Compaction

Vibro compaction uses an electric or hydraulic powered vibroflot suspended from a crane (Figure 25). The vibroflot consists of a torpedo shaped horizontally vibrating probe that vibrates at a frequency of 30 to 50 Hz with amplitude between 8 mm and 48 mm. By shearing of particles caused by the horizontal vibration, the loose soil particles are re-arranged into a denser configuration.

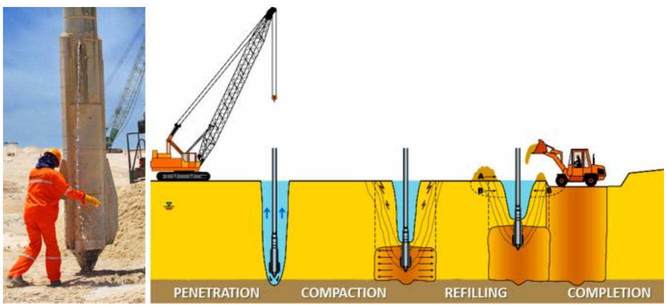

Figure 25 Vibroflot and different phases of vibro compaction

For sand compaction, it is recommended to use low frequency vibroflot with large amplitude to transfer the compaction energy generated by the vibroflot to the surrounding sand as efficiently as possible. This is achieved when the vibroflot is vibrating at 15 to 20 Hz in resonance with the surrounding sand. Resonance between the vibroflot and the sand leads to amplification of the ground vibrations, as the vibroflot and sand move "in-phase" with little or no relative displacements occurring. Water jet is used as a cutting medium to break up the sand mass during compaction. A water/air mixture is better than water jet alone. However, the drawback of using water/air jet is that the dissipation time may be longer and post compaction tests (e.g. CPT) may be influenced by air bubbles. Figure 26 shows a design chart with different vibroflot capacity (30 – 235 HP units). With larger vibroflots, the spacing between compaction points can be wider and productivity is improved.

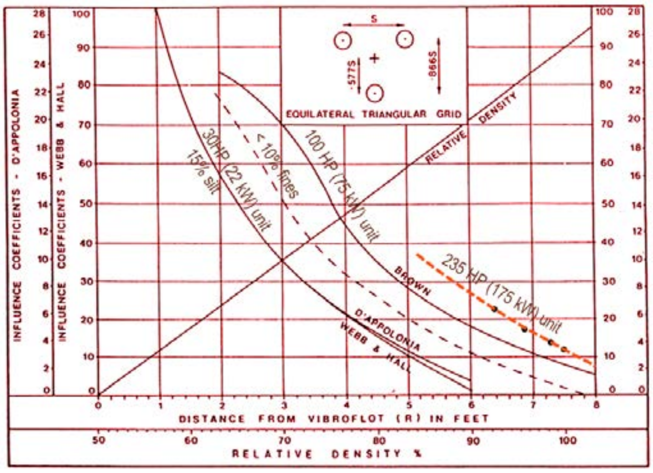

Figure 26 Vibro compaction spacing chart

4.4 Onshore Vibro / Dynamic Compaction Works

Deep compaction was carried out behind the seawall using vibro compaction and dynamic compaction to densify the hydraulic sand fill. Figure 27 shows the extent of the deep compaction works.

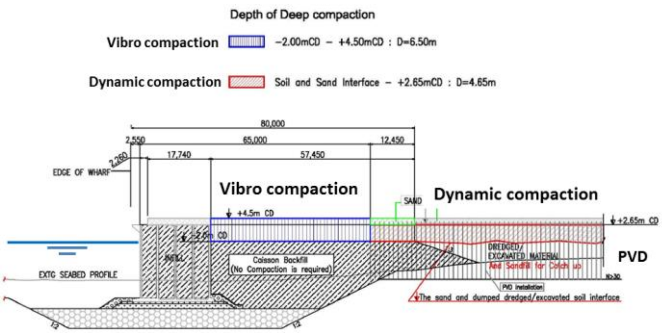

Figure 27 Cross-section of deep compaction area

The selection of the deep compaction technique was based on their inherent merits and constraints. Dynamic compaction has higher productivity and hence, a lower operating cost compared with vibro compaction. Hence, it is a financial advantage to use this technique. However, due to higher energy impacts on the ground surface dynamic compaction generates higher surface vibration than vibro compaction. For the fear of possible damage to the caisson seawall due to excessive ground vibrations, vibro compaction was carried out closer to the seawall. But, vibro compaction produces lesser degree of compaction at shallower depth compared with dynamic compaction due to lack of overburden pressure. Hence, an overburden fill of 1.5m was placed above the top finished level so that the upper layer can be sufficiently compacted using vibro compaction. Figure 28 summarises the key characteristics of the two deep compaction techniques.

A field vibration monitoring program was carried out to measure the ground vibrations in terms of the peak particle velocity (PPV). Different compaction energy per blow for dynamic compaction and different capacity vibroflots for vibro compaction were used. For dynamic compaction, an open cut trench of 1 – 1.5m deep was dug to cut-off the transmission of surface vibration to the seawall. The results are shown in Figure 29. A safe PPV of 4 mm/s for the seawall was adopted. A safe distance of 45m from the caisson seawall was demarcated for vibro compaction. Beyond 45m distance, dynamic compaction was carried out (Figure 27).

At the vibro compaction area, compaction commenced from elevation +4.5m CD to -2.0m CD i.e. 6.5m compaction. The working platform was raised to +6.0m CD to allow for the 1.5m overburden fill. At the dynamic compaction area, compaction commenced at +3.1m CD with compaction measured from +2.65m CD to -2.0m CD i.e. 4.65m compaction. The working platform was raised to +3.1m CD (i.e. 0.45m above top finished level) to allow for settlement compensation after compaction. The area of compaction was approximately 320,766 m^2 for vibro compaction and 1,572,127 m^2 for dynamic compaction. Hence, the total area for deep compaction of hydraulic sand fill was close to 1.9 million m^2.

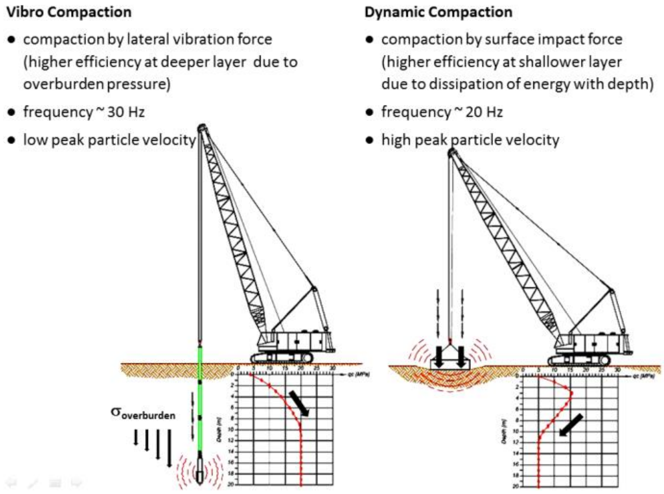

Figure 28 Characteristics of vibro compaction and dynamic compaction

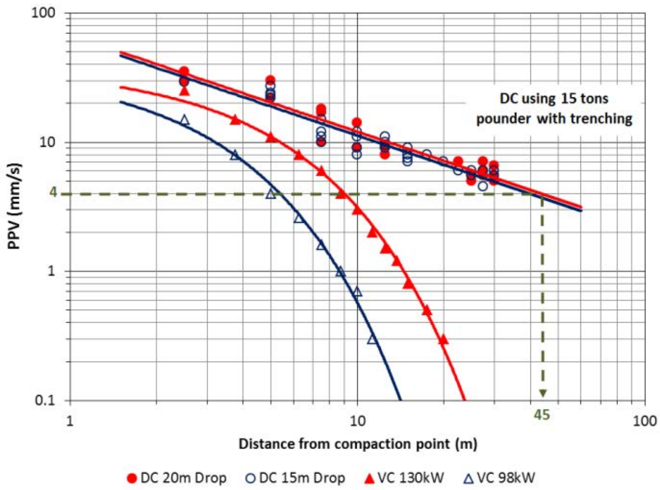

Figure 29 PPV measurements for dynamic compaction and vibro compaction

4.5 Performance Requirements

The performance criterion for deep compaction was relative density (D_R) of minimum 70%. The acceptance criteria based on cone penetration test (CPT) was cone resistance, q_c as shown in Table 5.

Table 5 Acceptance cone resistance (q_c) after compaction works

Description	Min. q_c
At 1 m below surface	6 MPa
At 2 m below surface	9 MPa
Between 2 to 3 m below surface	10 MPa
Between 3 to 4 m below surface	11 MPa
Between 4 to 7 m below surface	13 MPa

4.6 Field Calibrations

For deep compaction works, preliminary compaction spacing and working parameters are usually determined from past experiences and empirical design charts. Prior to actual production works, these parameters are established and confirmed following the completion of field calibrations (or "field trials"). The following parameters were used in a calibration area of 30m by 30m (900 m^2):

For calibration of dynamic compaction (DC) works:

- Working platform was at +3.1m CD (i.e. 0.45m above top finished level at +2.65m CD to allow for settlement).
- Spacing of compaction points was 6m square grid with two phases of compaction.
- Phase 1 consisted of 8 blows with 300 ton.m energy per blow (total energy per phase of 2,400 ton.m)
- Phase 2 consisted of 6 blows with 300 ton.m energy per blow (total energy per phase of 1,800 ton.m)
- Total applied compaction energy of 117 ton.m per m^2
- Treatment depth was 4.65m; measured from +2.65m CD to -2.0m CD

For calibration of vibro compaction (VC) works:

- Working platform was at +6.0m CD (i.e. 1.5m above top finished level at +4.5m CD as overburden fill).
- Spacing of compaction points was at an equivalent of 3.4m triangular grid using an electric vibroflot of 130 kW; 30 Hz frequency; 23mm amplitude with 30 ton centrifugal force. A combination of compressed air (using a 12,000 l/min compressor) and high pressure water jet (100 m^3/h under 1.2 MPa pressure) was used as cutting medium.
- Compaction was carried out to reach amperage of 200 amps or 40 seconds per 50cm lift whichever comes first.
- Treatment depth was 6.5m; measured from +4.5m CD to -2.0m CD

The above operation parameters were expected to meet the required acceptance q_c values.

4.7 Post Compaction Results

The post compaction results consisted of CPT results and enforced settlement measurements.

4.7.1 CPT results

Typical pre and post-compaction CPT results for vibro compaction and dynamic compaction are shown in Figures 30 and 31 respectively. Pre-compaction CPTs were carried out after the removal of surcharge fill. Profiles of relative density of 30%, 50% and 70% have been superimposed using the method of Baldi *et al.* (1982). The relative densities below water level varied between 30% and 60%, confirming a loose state. Above water level, it was in a denser state. The results also identified a layer of 0.5 to 1m thick dense sand at +3.5m CD i.e. about 1.5m above water level. This was the working platform for vertical drains installation and construction traffic to place surcharge fill – both had caused surface compaction.

The post-compaction CPTs were carried out 7 days after compaction. Above water level where the sand was initially in a denser state, the compaction did not show much improvement. The greatest improvement was below water level where the initial relative density was low (≤ 50%). However, it was noted that the post-compaction q_c values were at best only about 60% of the acceptance values – an unexpected large non-conformance!

4.7.2 Enforced Settlements

During dynamic compaction works, subsidence craters up to 3.5m in diameter were formed with penetration averaging 35cm per blow using a 1.83m x 1.83m steel pounder weighing 15 tons falling from 20m height. Water was frequently observed inside the craters. During vibro compaction works, subsidence craters up to 2.5m in diameter were formed around the shaft of the vibroflot. These subsidence craters were formed as a result of the densification of sand. These craters were then backfilled with sand on the surface.

Enforced settlement is the difference between the measured surface elevations before and after compaction. It is expressed as a percentage of the thickness of compactible sand layer. For dynamic compaction, the enforced settlement is computed from its working platform at +3.1m CD while for vibro compaction, it is computed from +4.5m CD where the compaction commenced. The upper 1.5m was not compacted as it was only an overburden fill. Compaction stopped at -2.0m CD. Any non-compactible interbedded cohesive layer within the sand fill mass is not included in the net thickness. Table 6 shows the measured enforced settlements.

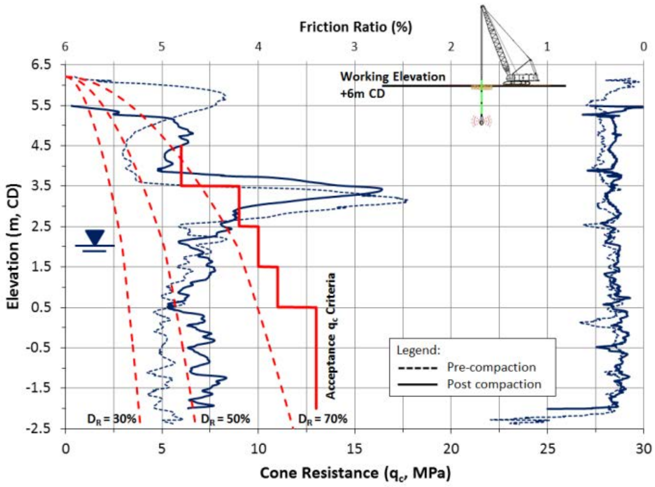

Figure 30 Pre and post CPT results for vibro compaction

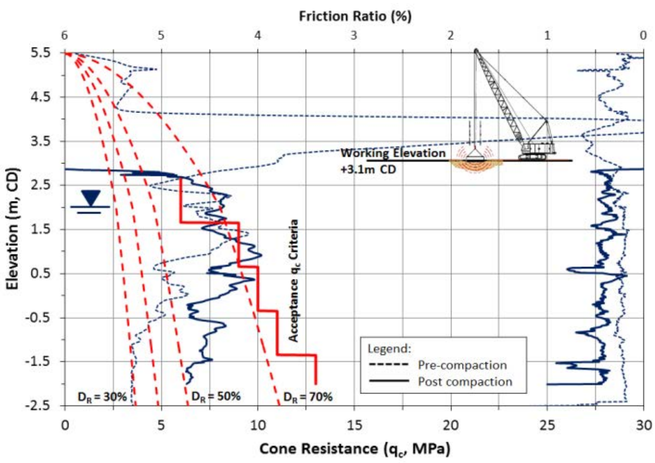

Figure 31 Pre and post CPT results for dynamic compaction

Table 6 Measured enforced settlements after VC/DC compaction

Methods	Net thickness of sand layer (m)	Enforced Settlement	
		(cm)	(%)
Dynamic compaction	3 – 5.1	25 – 40	7.8 – 8.3
Vibro compaction	5 – 6.5	50 – 60	7.7 – 12

4.8 Observations and Discussions

The unexpected large non-conformance of q_c values after VC/DC compaction was studied and presented below.

4.8.1 Estimation of relative density after VC/DC compaction

Enforced settlement is a function of initial relative density, thickness of sand layer and degree of improvement. From an assumed initial relative density, a final relative density can be estimated from the enforced settlement. The limitation with this method is that the initial relative density has to be estimated, and the values for minimum and maximum density may not be valid for the full thickness of the sand fill. Nevertheless, this method is a useful tool to use and may provide an insight to the non-conformance.

Undisturbed samples were collected after the removal of surcharge fill but prior to compaction. Laboratory tests were carried out following BS 1377 Part 4 1990 (Methods of tests for soils for civil engineering purposes: compaction-related tests). The minimum dry density varied from 1.31 to 1.33 Mg/m^3 with an average of 1.32 Mg/m^3 (12.9 kN/m^3). The maximum dry density varied from 1.75 to 1.83 Mg/m^3 with an average of 1.80 Mg/m^3 (17.6 kN/m^3). The specific gravity was 2.65. Using Equation (6), the calculated minimum void ratio varied from 0.45 to 0.51 with an average value of 0.48. The calculated maximum void ratio varied from 0.99 to 1.02 with an average value of 1.01. The following equations were used to determine the final relative density:

$$e = \frac{G_{s,}\gamma_w}{\gamma_d} - 1 \tag{6}$$

$$D_R = \frac{\gamma_{d,max}(\gamma_d - \gamma_{d,min})}{\gamma_d(\gamma_{d,max} - \gamma_{d,min})} \tag{7}$$

$$D_R = \frac{e_{max} - e}{e_{max} - e_{min}} \tag{8}$$

$$V_S = \frac{V_T}{1+e} \tag{9}$$

where D_R = relative density
e = void ratio
G_s = specific gravity (= 2.65)
γ_w = unit weight of water (= 9.8 kN/m^3)
γ_d = dry density
$\gamma_{d,max}$ = maximum dry density (= 17.6 kN/m^3)
$\gamma_{d,min}$ = minimum dry density (= 12.9 kN/m^3)
e_{max} = maximum void ratio (= 1.01)
e_{min} = minimum void ratio (= 0.48)
V_S = volume of solid
V_T = total volume

Based on the assumption of 45% initial relative density and using the enforced settlements of Table 6, the calculated relative densities after VC/DC compaction exceeded the 70% criterion (Table 7). This contradicts the non-conformance described earlier and it could not possibly provide any reasonable explanation.

Table 7 Calculated relative densities after VC/DC compaction

Methods	Enforced Settlement (%)	Relative Density (%)
Dynamic compaction	7.8 – 8.3	71.2 – 72.9
Vibro compaction	7.7 – 12	70.9 – 85.3

How reasonable is the assumption of 45% initial relative density? Radio-isotope (RI) cone penetrometer tests were carried out at an adjacent area. Relative densities below water were reported to be as low as 50%. Choa *et al*. (1979) reported relative density of hydraulic sand fill ranging from 40% to 80% at the Changi Airport reclamation. The lower values were obtained below water. Chu (2011) reported minimum relative density of 45% to 50% for the hydraulic sand fill at the Changi East reclamation. Figures 30 and 31 indicated relative density before compaction between 30% and 60% below water when interpreted using the method of Baldi *et al.* (1982). Hence, the assumption of 45% is not at all unreasonable.

4.8.2 Increased compaction energy

Is the applied compaction energy adequate? Causes of an inadequate compaction for vibro compaction works include larger spacing of compaction points, insufficient water/air jetting pressure and quicker withdrawal of vibroflot during compaction (inadequate compaction time). For dynamic compaction works, it includes inadequate total applied compaction energy per m^2, compaction energy per blow and insufficient rest period between phases of compaction.

To address these issues, additional field calibrations were carried out. For dynamic compaction, a 3rd phase compaction was carried out with additional 6 blows of 300 ton.m energy. The total applied compaction energy increased from 117 ton.m/m^2 to 167 ton.m/m^2 – an increase of 43%. The heave and penetration tests showed the penetration per blow was about 10 – 20cm for the 1st two blows and reduced rapidly to less than 10cm thereafter accompanied by substantial surface heaving around the craters. This suggested that the energy saturation point has been reached and further increase in the number of blows will only cause volumetric displacement (surface heaving) with no further densification in the soil mass.

For vibro compaction, the compaction grid of equivalent 3.4m triangular spacing was reduced to 3.1m – a 17% reduction in area coverage per compaction point. Varying duration of compaction and withdrawing criteria together with different combination of water/air jetting pressures were carried out in the new field calibration.

To account for "ageing" effect (i.e. increase of q_c with time), CPT tests were carried out 7, 14 and 21 days after compaction.

All the above produced little improvement (< 10%) and did not meet the acceptance q_c values. It was true that the operating parameters were optimised. Inadequate compaction was not the cause for the non-conformance. The only probable reason left was down to the intrinsic property of the sand fill material itself.

4.8.3 Carbonate content

Sand with significant carbonate content usually has higher initial void ratios and lower dry densities as a result of its angularity, poor grading and intra-particle porosity. The values of e_{min} (0.48) and e_{max} (1.01); and $\gamma_{d,min}$ (12.9 kN/m^3) and $\gamma_{d,max}$ (17.6 kN/m^3) when compared with typical values of silica sand fit into this trend (Table 8). These initial void ratios are comparable with carbonate sand found in Hong Kong and Dubai where e_{min} = 0.5 and e_{max} = 0.95 are average values for carbonate content greater than 10% (Figure 32).

Table 8 Typical void ratios and dry densities of sand (Das, 2008) compared with hydraulic sand fill (of this case study)

Soil Type	Void Ratio		Dry Density (kN/m^3)	
	e_{min}	e_{max}	$\gamma_{d,min}$	$\gamma_{d,max}$
Coarse sand	0.30	0.74	14.9	19.3
Fine sand	0.40	0.85	14.1	18.5
Hyd. sand fill	0.48	1.01	12.9	17.6

Samples were taken for laboratory tests following BS 1377 Part 3 1990 (Methods of test for soils for civil engineering purposes: chemical and electro-chemical tests). Visual inspections revealed the presence of calcitic shell fragments that were platy, flaky and porous. The test results confirmed carbonate content ranging from 13.1% to 15.2%. Chang *et al* (2006) reported a carbonate content of 8% to 16% in the direct-dumped sand and 4% to 12% in the hydraulic filled sand used in Changi East reclamation. Figure 32 shows carbonate sand found in Hong Kong, Changi (Singapore) and Dubai. The test results agreed with the trend shown.

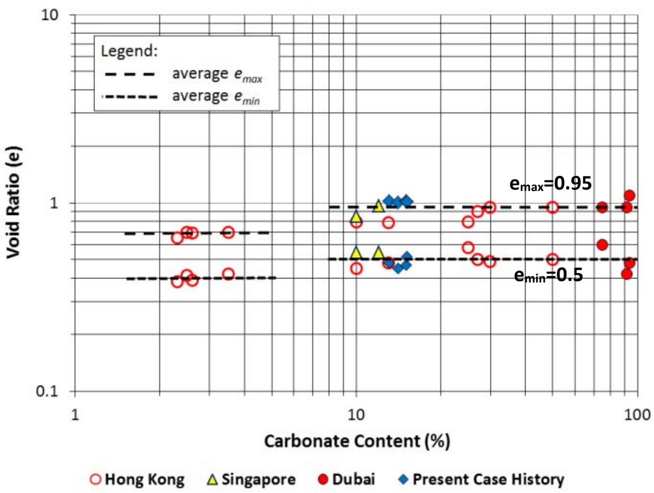

Figure 32 Void ratios of carbonate sand

4.8.4 Performance of carbonate sand

The performance of carbonate sand is strongly influenced by the crushability and angularity of the fragile carbonate grains, high initial void ratio of the fill and cementation between particles. Carbonate sand is susceptible to particle crushing and hence, it is more compressible than silica sand. For an equivalent relative density, the q_c values measured in carbonate sand will be less than in silica sand. Vesic (1965) added 10% shells to silica sand and resulted in a decrease of q_c values by a factor of 2.3. The higher crushability of the carbonate grains is responsible for the low q_c values. Since grain crushing increases with increasing density and increasing pressure therefore, a larger ratio of $q_{c(silica)}$ / $q_{c(carbonate)}$ is obtained for denser states and larger mean pressures. At a denser state, silica sand shows significant increase in q_c values since the hard particles are forced aside during cone penetration while for carbonate sand, it implies grain breakage, fracturing and crushing as the fragile particles are pushed closer together as they approach their minimum packing arrangement (i.e. e_{min}). Figure 33 presents test results that reflect this behaviour. When relative density is less than 30% (loose state), the measured q_c is about the same for both carbonate and silica sand. However, for relative density greater than 30% and increasing, the $q_{c(silica)}$ / $q_{c(carbonate)}$ increases significantly to reach a maximum value of 3.5 when the relative density is approaching 100%.

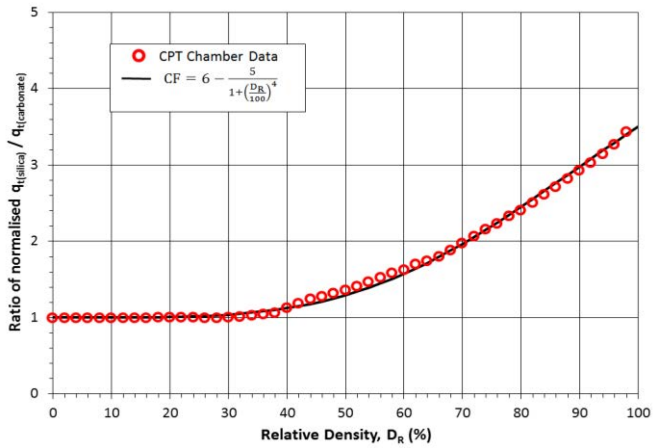

Figure 33 Ratio of $q_{c(silica)}$ / $q_{c(carbonate)}$ against D_R (Mayne, 2014)

In order to correctly assess the relative density of carbonate sand, correction factors (also known as "shell factors") are used to increase the q_c values of carbonate sand to equivalent values representative of silica sand and thus, allowing for the use of existing correlations (e.g. Baldi *et al.*, 1982) developed for silica sand. The correction factor given in Figure 33 is based on Kulhawy & Mayne (1990) and Jamiolkowski *et al* (2001) and it is expressed based on normalised cone resistance q_c values:

$$\frac{q_{c\,(silica)}}{q_{c\,(carbonate)}} = 6 - \frac{5}{1+(D_R/100)^4} \qquad (10)$$

Figures 34 and 35 show the post compaction q_c values adjusted with a correction factor of 2 following Equation (10) and Figure 33. With this correction, the measured equivalent q_c values satisfied the acceptance q_c values.

Also, profiles of relative density of 70% based on the method of Jamiolkowski *et al.* (1985) which was developed for various compressibility of sand are included in Figures 34 and 35. Sand of high compressibility includes carbonate (calcareous) sand while sand of intermediate (medium) compressibility includes siliceous sand with approximately equal parts of quartz and feldspar. Sand of low compressibility includes those of quartz. For high to intermediate compressibility, the measured q_c values meet the 70% relative density criterion after compaction. Hence, the carbonate content and its compressibility may have caused the unexpected large non-conformance of the results.

4.9 Lessons Learned

The question is "Is relative density a suitable performance (acceptance) criterion for deep sand compaction?" The degree of compactness of sand has been traditionally expressed in terms of relative density. In simple terms, it is merely the location of the void ratio (e) relative to its maximum (e_{max}) and minimum (e_{min}) values as expressed in Equation (8). The complication with the use of relative density is the difficulties in measuring density below water and the uncertainty associated with the determination of e_{max} and e_{min}. Hence, direct testing of relative density measurements is seldom used these days in favour of correlations developed from in-situ tests such as CPT.

Jamiokowski *et al.* (2001) reviewed test data obtained from calibration chamber tests (Figure 36). Supplemented with few data available on undisturbed frozen sand samples, it shows the relative density against the log scale of normalised cone resistance is almost a linear relationship but still exhibit quite a wide spread of data.

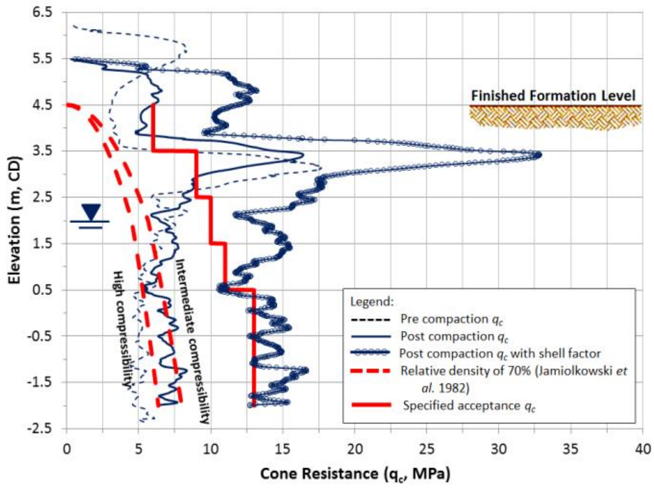

Figure 34 Cone resistance q_c and relative density for vibro compaction

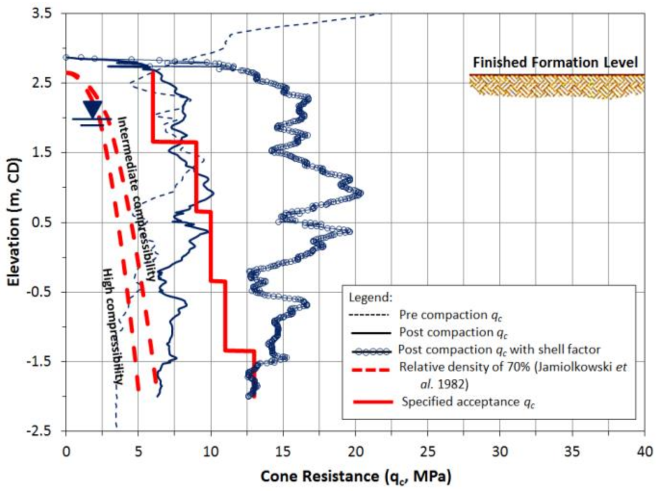

Figure 35 Cone resistance q_c and relative density for dynamic compaction

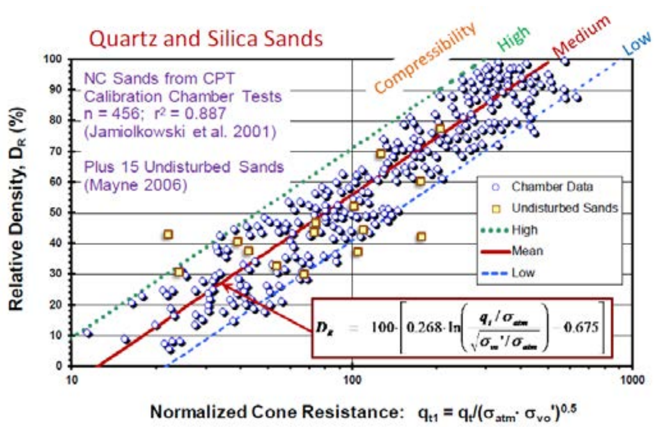

Figure 36 Relative density evaluations from CPT (Mayne, 2014)

For example, a normalised cone resistance of 100 would give a relative density ranging from 40% to 70% depending on the compressibility of sand. Also, there is a big spread for the undisturbed samples e.g. a 40% relative density would have a normalised cone resistance from 20 to 200. Hence, a q_c reading can correspond to a large range of relative densities and this leads to uncertainty in the estimation of a "true" relative density.

The uncertainty gets worse with carbonate sand. Although some correction factors have been proposed to "correctly" assess the relative density of carbonate sand from existing standard correlations for silica sand, these factors are varying over a range of values. This increases the uncertainty already associated with the standard correlations. Therefore, the concept of relative density may not be suitable to be used in the specifications for deep sand compaction in land reclamation projects especially sand fill with substantial carbonate content.

It would be more appropriate to derive "directly" the specifications according to performance criteria which are established from the functional requirements of the project needs – defined by the allowable stress-induced deformation (stiffness), bearing capacity and stability requirements (strength) and liquefaction potential. It is noted that relative density is an intermediate parameter. Strength and stiffness are not always well represented by relative density. In contrast, the cone resistance (q_c) is essentially directly responding to both the strength and stiffness. The measurements of cone resistance, sleeve friction and pore water pressure can be used either separately or together to evaluate soil engineering parameters including state of stress, strength and stiffness. Thus, it is far better to estimate the friction angle, stiffness and liquefaction directly from CPT results and not go through the intermediary step of using relative density to estimate these soil engineering parameters. Instead of stipulating the relative density and the accompanying test values (e.g. CPT q_c) in the specifications, it is far better to stipulate the required stiffness and strength parameters. Recently, the state parameter (Ψ_S) has found interest because of its application to critical soil mechanics and a rational framework towards understanding of soil liquefaction problems.

5. CONCLUSIONS

The quest for land is as old as time immemorial. Land is Singapore's most cherished resource. Since its first land reclamation works in 1822, the small city-state has grown from 58,150 to 71,910 hectares in 2017. It has set a goal to reach 76,600 hectares by 2030. This whopping increase in land area by reclamation – dubbed by the local media as a "gift from the sea"; brought many challenges and also opportunities for innovative solutions.

Some of the challenges and lessons learned in soil improvement works and acceptance tests are highlighted in this paper. The following lessons learned by the authors have been discussed:

- Adaptation of non-conventional materials to be used for soil improvement works in deep water under the prevailing conditions to achieve the required performance criteria;
- Adaptation of "site-specific-designed" construction plant and equipment used for the soil improvement work in deep water;
- Use of appropriate quality control (QC) in-situ tests (e.g. static and cyclic PMT tests) to suit the type of materials to be tested;
- Conduct visual inspections and field observations (especially in deep water) before, during and after works to provide additional information to supplement results obtained from in-situ tests.
- Specify performance criteria that are established from functional requirements of the project needs defined by soil engineering parameters.

The authors believe that successful soil improvement requires a blend of relevant soil engineering parameters, informed analytical modeling supported with appropriate methods of analysis, adequate in-situ and laboratory tests coupled with field observations and performance measurements according to functional performance criteria. Learning and heeding lessons learned from past projects are important additions to the list.

6. ACKNOWLEDGMENTS

The authors wish to thank their former colleagues in Menard for their assistance with some of the works described in this paper. They also wish to record their gratitude and admiration to the project owner, project consultants, project managers and main contractors who have given them the opportunity to work on this challenging project and wish to thank them for their insight and dedication to excellence in dealing with the project's technical challenges.

7. REFERENCES

Amar, S., Clarke, B.G.F., Gambin, M.P. and Orr, T.L.L. (1991). The Application of Pressuremeter Test Results to Foundation Design in Europe. Part 1: Predrilled Pressuremeters / Self-boring Pressuremeters. ISSMFE European Regional Technical Committee No. 4 – Pressuremeters. 48 p.

Baldi G., Bellotti R., Ghionna V., Jamiolkowski M. and Pasqualini E. (1982) "Design parameters for sands from CPT", Proceedings of the 2nd European Symposium on Penetration Testing, ESOPT II, Amsterdam, May, Vol. 2, pp. 427 - 432.

Chang M.F., Yu G., Na Y.M. and Choa V. (2006) "Evaluation of relative density profiles of sand fill at a reclaimed site" Canadian Geotechnical Journal, Vol. 43, pp. 903 - 914.

Choa V., Karunaratne G.P., Ramaswamy S.D., Vijiratnam A. and Lee S.L. (1979) "Compaction of sand fill at Changi Airport", Proc. of the 6th Asian Regional Conference on Soil Mechanics & Foundation Engineering, Singapore, Vol. 1, pp. 137 - 140

Chu J. (2011) Personal Communications.

D'Appolonia E. (1970) "Dynamic loading", Journal of Soil Mechanics & Foundation Engineering, ASCE Vol. 96 No. SM1.

D.60.AN (1975). The Menard Pressuremeter – Interpretation and Application of Pressuremeter Test Results to Foundation Design. General Memorandum. Sols –Soils No: 26 45 p.

Das B. M. (2008) Advanced Soil Mechanics, Taylor & Francis, London & New York.

Jamiolkowski M., Ladd C.C., Germaine J.T. and Lancellotta R. (1985) "New developments in field and laboratory testings of soils", State-of-the-Art Report. Proceedings of the 11th ICSMFE, San Francisco, Vol. 1 pp. 57 - 153.

Jamiolkowski M., LoPresti D.C.F. and Manassero M. (2001) "Evaluation of relative density and shear strength of sands from cone penetration test and flat dilatometer test", Soil Behaviour and Soft Ground Construction, GSP 119, ASCE, Reston, VA, pp. 201 - 238.

Kulhawy F.H. and Mayne P.W. (1990) "Estimating soil properties for foundation design", EPRI Report EL-6800, Electric Power Research Institute, Palo Alto, 306 p.

Mayne P.W. (2014) "Interpretation of geotechnical parameters from seismic piezocone tests", Proc. 3rd International Symposium on Cone Penetration Testing, Las Vegas, Nevada, pp. 47-73

Menard, L. (1970). Determination de la Poussee Exercee par un Sol sur une Paroi de Soutenement. Centre d'Etudes Menard, Publication D.38. 1970.

The Straits Times (2016) "Engineering feats at Pasir Panjang a model for Tuas" October 28, 2016

Varaksin, S. and Racinais, J. (2009) "Etude Des Paramètres D'application de la Consolidation Dynamique et de ses Techniques Dérivées" Proceedings 17th ICSMGE, Alexandria, Egypt, pp. 2407 - 2410.

Varaksin, S. (2009). Personal Communications

Vesic A.S. (1965) "Ultimate loads and settlements of deep foundations in sand" Proceedings of the Symposium on Bearing Capacity and Settlement of Foundations in Sand, Duke University, Durham, pp. 53-68

Yee, K and Varaksin, S. (2012) "Ground Reinforcement in Deep Water" Proceedings of the International Conference on Ground Improvement and Ground Control, Wollongong, Australia 30 Oct – 2 Nov 2012, pp. 575 - 585